Journal of Biological Control, 38(1): 29-40, 2024, DOI: 10.18311/jbc/2024/36151

Research Article

Evaluating the efficiency of silver nanoparticles prepared using *Pseudomonas fluorescens* and *Bacillus thuringiensis* subsp. *tenebrionis* in controlling eggs and adults of *Callosobruchus maculatus* (F.) (Coleoptera: Bruchidae)

ISTABRAQ F. ALI[1]*, RAGHAD K. I. AL-JOBOORY[1] and HAZIM I. AL-SHAMMARI[2]
[1]*Department of Biology, College of Education, University of AL-Iraqia, Baghdad, Iraq*
[2]*Department of Agricultural Research Integrated Pest Control Center, Ministry of Science and Technology, Baghdad, Iraq*
**Corresponding author E-mail:* istabraq.fouad96@gmail.com

ABSTRACT: This study aimed to evaluate the efficiency of silver nanoparticles (AgNPs) which are prepared biologically by two bacterial species, *Bacillus thuringiensis tenebrionis* (*Btt*) and *Pseudomonas fluorescens* (P.f) to control southern cowpea beetle insect, *Callosobruchus maculatus*. Many features of the prepared nanoparticles were examined, and the results obtained showed that the highest absorption value of AgNPs was at 262 nm. Whereas the results of FTIR analysis showed that several compounds played a role in the silver ions reduction process, which included alcohol, alkane, primary amine, and amine group. The scanning electronic microscopic images showed that the average diameter of nanoparticles which was created by P.f was 48.52 nm, while it was 56.08 nm for the nanoparticles prepared by *Btt*. The study showed no significant differences between the activity of both AgNP types against *C. maculatus* eggs, while a significant preference was recorded for the activity of *Btt* AgNPs against the *C. maculatus* adults. The highest percentage of unhitched eggs was 53.8% recorded at 3000 ppm concentration, while *Btt* AgNPs gave 59.6% at 3000 ppm. The highest mortality rate of the adults who were treated by *Btt* AgNPs was 58.8 % at 3000 ppm concentration, while it was recorded 50% at 3000 ppm with P.f AgNPs treatment. The current study demonstrates the efficiency of biologically prepared AgNPs in controlling *C. maculatus* insect life stages, which encourages using of these nanoparticles as a modern strategy in management of insect pests.

KEYWORDS: Biological control, *Callosobruchus maculatus,* silver nanoparticles, toxicity

(Article chronicle: Received: 10-01-2024; Revised: 17-03-2024; Accepted: 20-03-2024)

INTRODUCTION

Callosobruchus maculatus is an agricultural pest that affects legumes, characterized by its widespread globally, as well as locally in Iraq causing significant losses in crops. The infections of these insects begin at the field, remains and transport even the seed stores, these insects prefer cowpea seeds over other types of legumes (Arora & Srivastava, 2020). The importance of the insect is related to its non-specificity, as it does not affect a specific type of legume plant, but its larvae can grow and develop in about 35 types of legume seeds (Neto *et al.*, 2019). Both quantitative and qualitative damages are caused by *C. maculatus*, it makes a hole in seeds, which decreases its weight, minimizes its marketing value, and reduces its germination potential (Kalpna & Kumar, 2022). The damage ratio of *C. maculatus* ranged between 30-40% within six months, but it can reach 100% if left without control (Majhi & Mogali, 2020). Many ways have been used by researchers to control the infections of *C. maculatus* including the application of chemical pesticides, and due to their rapid effectiveness, chemical pesticides represent the most common pesticide method. Despite their frequent use, most organic chemical pesticides are recorded as neurochemicals that affect the nervous system (Mohammed & Aswad, 2019). Chemical pesticides also have several environmental threats (Pisa *et al.*, 2021). Recently, nanotechnology emerged as a promising field of research with many applications in agriculture, like the use of nanoparticles (NPs) in curing plant diseases, improving agricultural production, as well as controlling pests (Match *et al*., 2018). Some NPs are highly efficient alternatives with low-cost production and Ecofriendly products, and due to their tiny sizes and large effective surfaces, NPs have different properties in comparison to properties of the original material from which they came (Sharma and Uttam, 2017). The biosynthesis of nanoparticles based on the utilisation of microorganisms or their by-products is more efficient than the chemical or physical methods. It is distinguished by its stability, less toxicity, environmentally friendly, and cheaper (Khan *et al*., 2018). Silver nanoparticles (AgNPs)

which are prepared by biological methods have received great attention due to their effectiveness in the biology, physics, and chemistry fields, as well as their activity against pathogens and various insect pests (Dakhil *et al*., 2017). Because of *C. maculatus* economic importance and the efficiency of bacterial pathogens as biological control agents with their role in preparing nanomaterials by safe methods, and in trying to find new combinations of pesticides within nanotechnology, we performed this study achieving the following goals: Preparation of AgNPs by *Pseudomonas fluorescens* and *Bacillus thuringiensis* subsp. *tenebrionis*, assessment of some of their characteristics, and evaluation of their activity against eggs and adults of *C. maculatus* in lab conditions.

MATERIALS AND METHODS

Collection and rearing of insects

For sample collection, *C. maculatus* was isolated from the infected red cowpea, which were collected from the local markets in Baghdad. The insects were then diagnosed in the Iraq Natural History Museum of Baghdad University. For breeding, an amount of intact and sterilized seeds was placed in each glass bottle (800 ml capacity), then several adult insects were added, the bottles were covered by wet clothes and tightly closed by rubber bands, then incubated at (30±2°C) and (70±5) humidity. These farms have been continuously renewed to preserve the insects until making the experiments (Mahmoud, 1989).

Bacterial strains

The two strains of *P. fluorescens* were isolated from *Locusta* and *Periplaneta americana*, diagnosed morphologically and molecularly by PCR while the local strain of *B.t. tenebrionis* was isolated from *Jebusaea hammerschmiditi*, also diagnosed morphologically and molecularly by PCR.

Preparation of AgNPs

At first, the nutrient broth was prepared by adding (13 g) of medium powder to (1000 ml) distilled water, dissolved and sterilized by autoclave (121°C, 15 bar, for 20 minutes). Then the prepared media were inoculated with the bacterial isolates separately and incubated at (2±27°C) for 48 h, after incubation the bacterial cultures were centrifuged for half an hour and the supernatant was obtained, while the sediment was discarded.

A concentration of (10 mmol/L) silver nitrate solution was prepared by dissolving 1.7 g of silver nitrate in 1000 ml deionized water in a dark place, to avoid Photo oxidation, and stored in the refrigerator until use. In the next step, 100 ml of bacterial supernatant (previously prepared) was added gradually to 900 ml of silver nitrate solution, pH was adjusted to 8.0, then the mixture was placed in a water bath for three hours and monitored continuously to observe the colour change until brown appearance. To obtain the NPs in powder, the mixture is centrifuged for half an hour, then the precipitated part is isolated and deionized water is added and re-centrifuged, this process is repeated 3 times. After that, the precipitated part was collected in Petri dishes and placed in the oven for 3 h at 80°C to dry, finally, the resulting powder was collected in an opaque glass container. (Al-Jaafari, 2022; Syed *et al*., 2016).

Determination of some properties and characteristics of prepared AgNPs

Some features of the prepared AgNPs were determined as follows, UV.VIS Spectrophotometer device was used to determine some optical properties of AgNPs and bacterial suspensions. Fourier Transform Infrared (FTIR) device was used to determine the functional groups of bacterial supernatant as well as AgNPs, while the shapes and diameters of AgNPs were detected by Field Emission Scanning Electron Microscope (Fe-SEM). Energy-dispersive X-ray spectroscopy (EDX) to determine elemental composition. The crystal sizes were detected by X-ray diffraction (XRD), Zetasizer device was also used for assessment The zeta potential of AgNPs was obtained (Stock, 2001; Thuy *et al*., 2021).

Evaluating the activity of AgNPs against the eggs of *C. maculatus*

The experiments were carried out using three different concentrations (1000, 2000, and 3000 ppm) for both kinds of AgNPs. Twelve plastic cans were prepared, each can provided by ten newly laid eggs (24 h), these cans were arranged as follows; three replicates for each concentration as well as the control treatment. The controls were treated with distilled water, the rest of the samples were treated directly by spraying, three times at a distance of 10 cm. The cans were then closed and holes were made in their covers for ventilation. After incubation, the hatched eggs and the % unhitching eggs were calculated according to the Abbott formula (Abbott, 1925).

$$\% \text{ unhitching eggs} = \frac{\text{No. of hatching eggs in control} - \text{No. of hatching eggs in treatment}}{\text{No. of hatching eggs in control}} \times 100$$

Evaluating the activity of AgNPs against the adults of *C. maculatus*

The experiments were also carried out using three different concentrations (1000, 2000, and 3000 ppm) for both kinds of AgNPs. Twelve plastic cans were prepared, each filled with 10 newly emerged adults and 10 healthy seeds.

Three replicates were made for each concentration, as well as the control. Treatment is done by spraying three times at a distance of 10 cm. Insect deaths were recorded daily for 96 hours after treatment. The corrected mortality rate of adults was calculated according to Abbott Formula (Abbott, 1925).

Statistical design and analysis

In this study, factorial experiments were performed according to a Completely Randomized Design (CRD), and the differences between The means treatments were compared according to the Least Significant Difference (LSD) at a probability level of 0.05. (Al-Sahoky & Wahayib, 1990). The results were analyzed using Genstat 12 software.

RESULTS

Determination of some properties and characteristics of prepared AgNPs

UV-Vis spectrophotometer analysis

The addition of bacterial extract to silver nitrate solution leads to a brown colour formation, which indicates the reduction of silver ions to Silver nanoparticles. Figure 1 shows the UV-Vis spectrophotometer analysis of *Btt* bacterial extract, where the highest absorbance appeared at 204 nm, and the highest absorbance of AgNPs which is prepared by the same bacterial extract was at 262 nm Figure 2, while the highest absorbance of P.f bacterial extract was at 236 nm, Figure 3, and the highest absorbance of AgNPs which is formed by these bacterial extract was at 262 nm, Figure 4. The absorbance peak of silver nitrate was at 228 nm, Figure 5.

FTIR analysis

Figure 6 and Table 1 show the FTIR results of *Btt* bacterial extract. The figure shows many peaks formed at the following regions (3774.95, 3436.28, 2928.56, 1989.86, 1629.65, 1399.25, 1234.64 and 1096.45) cm^{-1}, they represent the following active groups (alcohol group OH, aromatic compound CH, carboxylic acid OH, alkene C=C and amine group CH respectively. FTIR results of AgNPs that were

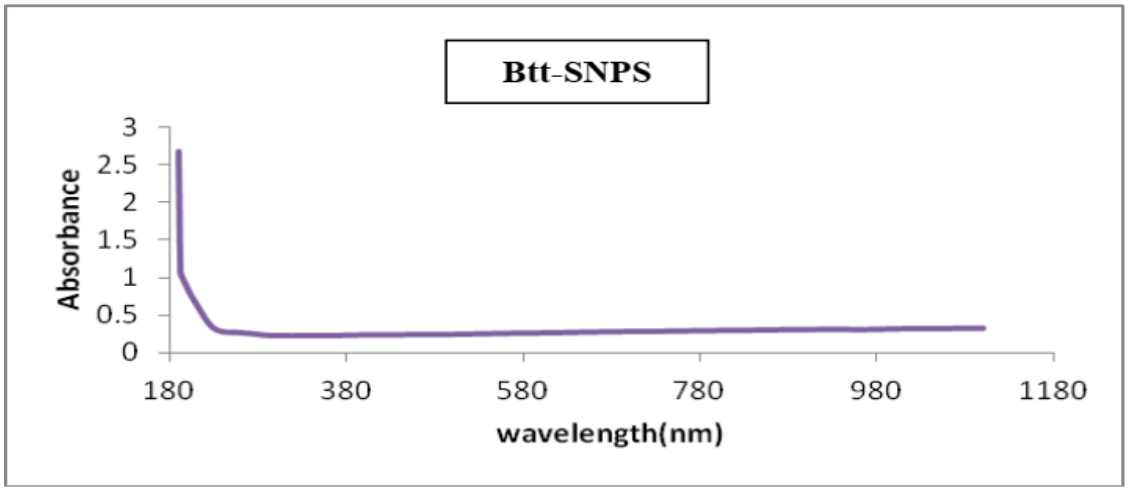

Figure 1. The absorption spectrum of local bacteria supernatant of *Bacillus thuringiensis* subsp. *tenebrionis.*

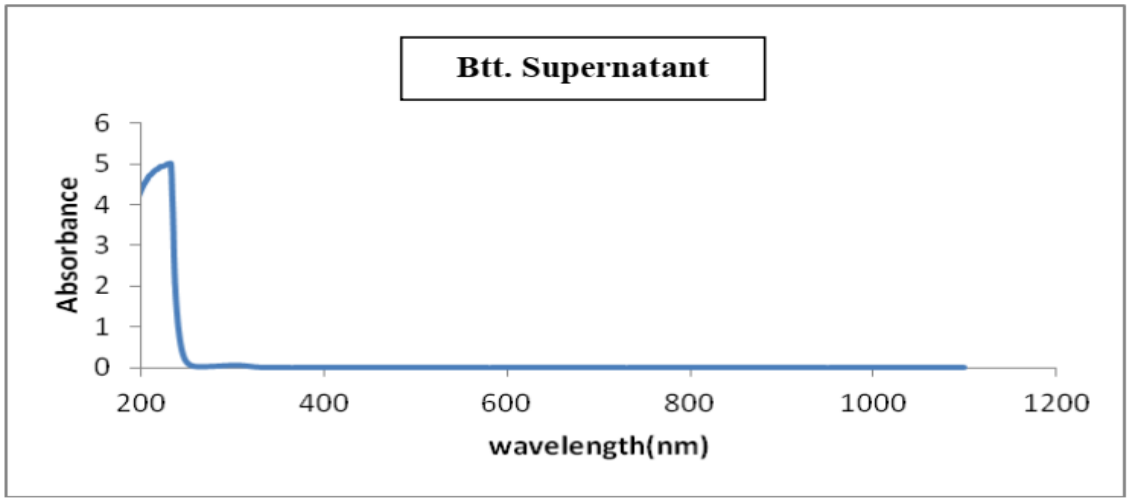

Figure 2. The absorption spectrum of silver nanoparticles prepared by isolating local bacteria *Bacillus thuringiensis* subsp. *tenebrionis.*

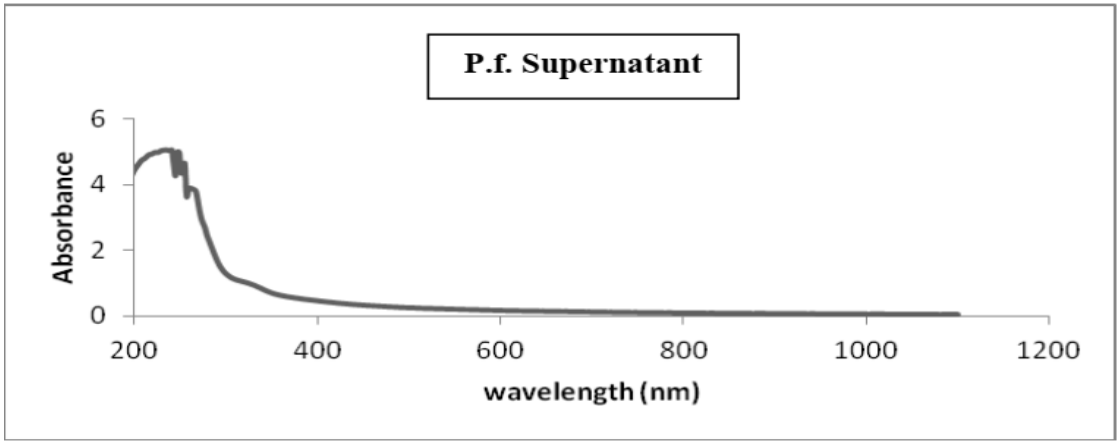

Figure 3. Absorption spectrum of local bacteria supernatant of *Pseudomonas fluorescens.*

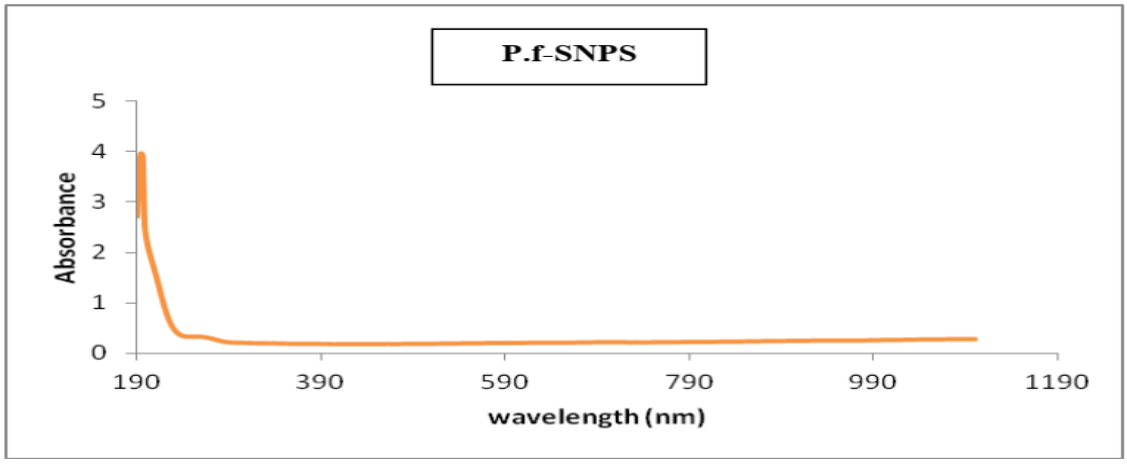

Figure 4. The absorption spectrum of silver nanoparticles prepared by isolating local bacteria *Pseudomonas fluorescens.*

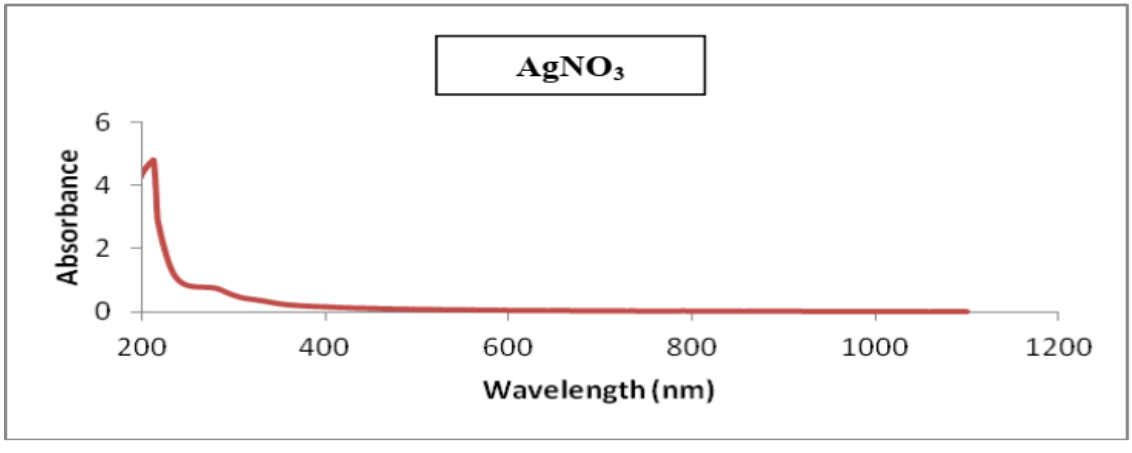

Figure 5. Absorption spectrum of $AgNO_3$.

prepared by *Btt* bacterial extract, where the peaks located at the regions (1107, 1458, 1631, 2667, 2924, 3435, 3776 and 3774.95) cm^{-1}, they represent the followings (alcohol group OH, alkane group CH, and amine group CN) respectively. Figure 7 and Table 2 show FTIR analysis of P.f bacterial extract, where the peaks appeared at (3437.10, 2066.13, 1636.63, 1461.05, 1411.02, 1099.18, 1075.38, 1031.14 and 691.70) cm^{-1}, which represent a following functional group (alcohol OH, isothiocyanate group N=C=S, amine group NH, alkane CH, carboxylic acid OH, amine C-N and alkane C=C respectively. They also show the FTIR analysis of AgNPs which were prepared by P.f bacterial extract, where the peaks appeared at the following regions (3436.49, 2066.47, 1636.85, 1404.15, 1363.09, 1101.08, 1076.20, 1031.02 and 990.90) cm^{-1}, and represent the following functional groups, respectively (alcohol OH, isothiocyanate, amine CN, carboxylic acid OH and alkene C=C), respectively.

Scanning Electron Microscope (SEM) analysis

Shapes and diameters of AgNPs were examined by the SEM at 100,000X. and Image j1.46r. Figure 8a is an image of P.f AgNPs, it is noted that the molecules were spherical and irregular, and no clusters were shown. Their diameters ranged between (43.99 and 54.33 nm), with an average of 48.58nm. The purity and concentration were measured by X-ray EDX device, and the results were shown in Figure 8b and Table 3. where the weight ratio of P.f AgNPs was 56.86%, and other elements were also detected like B = 10.90, C = 15.90, Cl = 16.33, these elements were formed by the secondary bacterial metabolites, which perhaps participated in the reduction and bioencapsulation of silver ions. Figure 8c represents the *Btt* AgNPs image. As shown in the image, the molecular weight of the NPs ranged between (43.24 and 72.05nm) with an average of 56.08 nm. They are semi-spherical and clear, and no clusters were found. Figure 8d and Table 3. represent the X-ray EDX analysis of *Btt* AgNPs, where the weight % reached 62.67%, and other elements were also detected (B = 6.62, C = 14.50, Cl = 16.20), these elements were formed by the secondary bacterial metabolites. According to the results, the prepared AgNPs fall within the nanoscale level, (as the particle sizes in the nanoscale ranged between 1-100 nm), which gives them new properties, they acquire unique physical, chemical and biological characteristics that are not present in the original materials from which they were made.

Crystal sizes of the prepared AgNPs

The X-ray diffraction analysis of *Btt* AgNPs is shown in Figure 9, there are eight Bragg angles (27.88 - 32.29 - 46.3 - 54.87 57.53 - 67.53 - 74.52 - 76.77°), while the total width is at the middle of the maximum value of the diffraction peak height (FWHM) were (0.2952 - 0.246 - 0.246 - 0.246 - 0.344 - 0.3936 - 0.393 - 60.24) respectively. The equation of Debye-Scherrer was applied to find the crystal sizes of AgNPs, and the average size was 32.79 nm.

The X-ray diffraction analysis of P.f AgNPs is shown in Figure 10, they are also eight Bragg angles which are (27.8869 -32.3004 -46.2964 - 54.8644 –57.5317 67.4985 – 74.5176 –

Table 1. Functional groups of bacterial local isolate supernatant and silver nanoparticles prepared by supernatant of *Bacillus thuringiensis* subsp. *tenebrionis*

Peak Number	*Bt*-extract	Functional groups	Class	*Bt*-SNPS	Functional groups	Class
	Wavenumber (cm^{-1})			Wave number (cm^{-1})		
1	3774.95	O-H stretching	alcohol	3917.36	O-H stretching	alcohol
2	3436.28	O-H stretching	alcohol	3778.62	O-H stretching	alcohol
3	2928.56	O-H stretching	alcohol	3435.23	O-H stretching	alcohol
4	1989.86	C-H bending	aromatic compound	2924.98	O-H stretching	alcohol
5	1629.65	C=C stretching	alkene	2857.27	O-H stretching	alcohol
6	1399.25	O-H bending	carboxylic acid	1631.28	C=C stretching	alkene
7	1234.64	C-N stretching	amine	1458.93	C-H bending	alkane
8	1096.45	C-N stretching	amine	1107.26	C-N stretching	amine

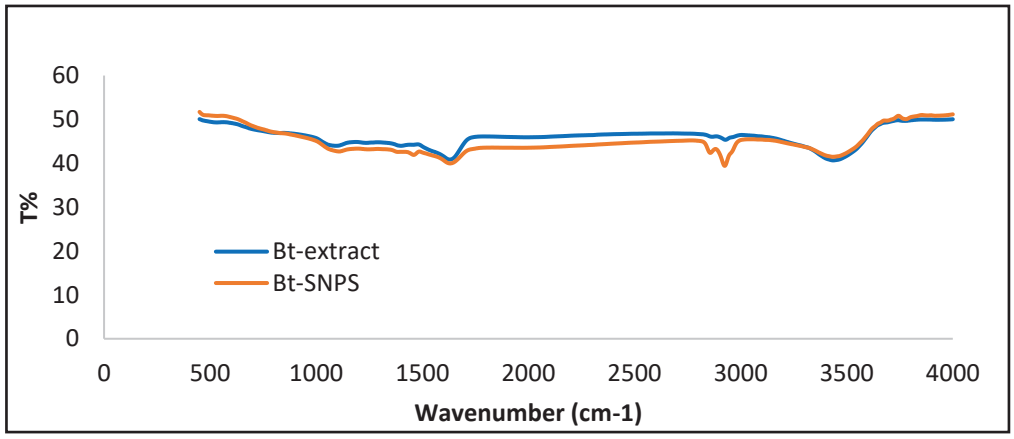

Figure 6. FTIR of bacterial local isolate supernatant and silver nanoparticles prepared by supernatant of *Bacillus thuringiensis* subsp. *tenebrionis*.

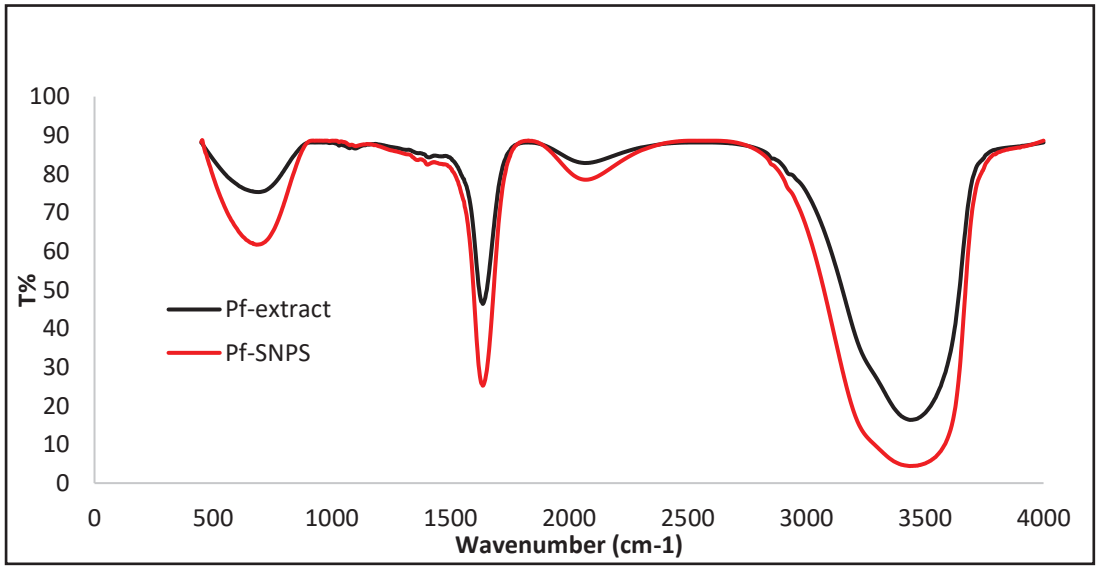

Figure 7. FTIR of bacterial local isolate supernatant and silver nanoparticles prepared by supernatant of *Pseudomonas fluorescens*.

Table 2. Functional groups of bacterial local isolate supernatant and silver nanoparticles prepared by supernatant of *Pseudomonas fluorescens*

Peak Number	Pf-extract Wavenumber (cm^{-1})	Functional groups	Class	Pf-SNPS Wave number (cm^{-1})	Functional groups	Class
1	3437.10	O-H stretching	alcohol	3436.49	O-H stretching	alcohol
2	2066.13	N=C=S stretching	isothiocyanate	2066.47	N=C=S stretching	isothiocyanate
3	1636.63	N-H bending	amine	1636.85	N-H bending	amine
4	1461.05	C-H bending	alkane	1404.15	O-H bending	carboxylic acid
5	1411.02	O-H bending	carboxylic acid	1363.09	O-H bending	alcohol
6	1099.18	C-N stretching	amine	1101.08	C-N stretching	amine
7	1075.38	C-N stretching	amine	1076.20	C-O stretching	primary alcohol
8	1031.14	C-N stretching	amine	1031.02	C-N stretching	amine
9	691.70	C=C bending	alkane	990.90	C=C bending	alkene

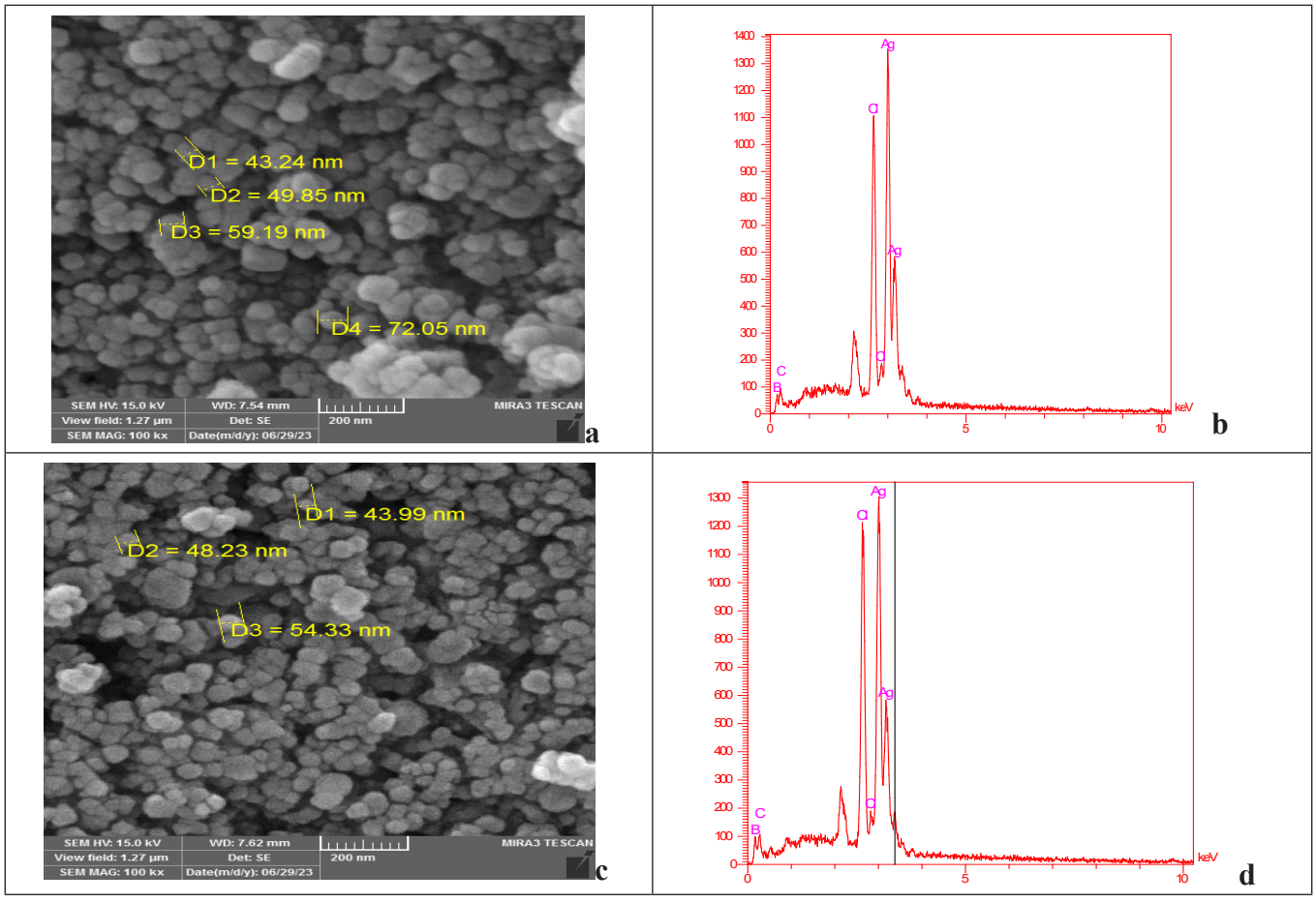

Figure 8. Scanning electron microscope images of silver nanoparticles prepared by *a: Pseudomonas fluorescens* c: *Bacillus thuringiensis* subsp. *tenebrionis* and EDX Analysis of silver nanoparticles prepared by b: *Pseudomonas fluorescens d: Bacillus thuringiensis* subsp. *tenebrionis.*

Table 3. EDX analysis of silver nanoparticles prepared by bacterial extract of *Bacillus thuringiensis* subsp. *tenebrionis*

Elt	Line	Int	Error	K	Kr	W%	A%	ZAF		Ox%	Pk/Bg	Class	LConf	HConf	Cat#
B	Ka	30.6	4.1779	0.0709	0.0565	6.62	21.43	0.8532		0.00	5.31	A	5.87	7.38	0.00
C	Ka	82.4	4.1779	0.0433	0.0345	14.50	42.25	0.2380		0.00	12.38	A	13.50	15.51	0.00
Cl	Ka	1026.5	1.8846	0.2118	0.1687	16.20	15.99	1.0417		0.00	22.30	A	15.88	16.52	0.00
Ag	La	1402.0	1.8846	0.6739	0.5369	62.67	20.33	0.8566		0.00	31.56	A	61.62	63.73	0.00
				1.0000	0.7966	100.00	100.00			0.00					0.00

Table 4. EDX analysis of silver nanoparticles prepared by bacterial extract of *Pseudomonas fluorescens*

Elt	Line	Int	Error	K	Kr	W%	A%	ZAF		Ox%	Pk/Bg	Class	LConf	HConf	Cat#
B	Ka	54.3	4.2758	0.1194	0.0921	10.90	30.38	0.8451		0.00	7.58	A	9.97	11.84	0.00
C	Ka	86.3	4.2758	0.0431	0.0332	15.90	39.87	0.2090		0.00	15.54	A	14.82	16.98	0.00
Cl	Ka	1108.8	2.0499	0.2171	0.1676	16.33	13.88	1.0259		0.00	24.35	A	16.03	16.64	0.00
Ag	La	1360.1	2.0499	0.6204	0.4788	56.86	15.88	0.8420		0.00	31.92	A	55.89	57.83	0.00
				1.0000	0.7717	100.00	100.00			0.00					0.00

76.7742 °), while the FWHM were (0.2952-0.2952-0.2952-0.3444-0.3444-0.3444-0.492-03) respectively. The average crystal size was 28.63 nm.

Zeta potential analysis

Figure 11 clarifies the zeta potential of *Btt* AgNPs, where the average zeta potential value was -50 millivolts, which indicates good stability. as the value of zeta potential reflects the stability of the particles and their less tendency to cluster. Figure 12 shows the zeta potential of P.f. AgNPs, where the average zeta potential was -57.2 millivolts. The results of the zeta potential analysis correspond with those of the scanning electron microscope, where the diameter of the particles was less than 100 nm and the shape was semi-spherical with no clusters.

Evaluating the activity of AgNPs against eggs of *C. maculatus*

The results recorded in Table 4 show the impact of different AgNP concentrations of both bacterial types on the hatching percentage. For what happened when the eggs were treated with P.f AgNPS, it is noted that the lowest ratio of unhatched eggs was 7.7% gained when using the treatment concentration of 1000 ppm, while the highest ratio of unhatched eggs was 53.8% at 3000 ppm. Regarding the treatments of *Btt* AgNPs, the lowest percentage of unhatched eggs was 11.5% at 1000 ppm, while the highest percentage of unhatched eggs was 59.6% at a concentration of 3000 ppm. The statistical analysis showed no significant differences between unhitched egg percentages when treated with both types of AgNPs. Statistical analysis also showed that the percentages of unhitched eggs increased with the concentration by a significant difference, with a preference for the 3000 ppm treatment. The statistical analysis indicated that the studied parameters did not affect the egg-hatching percentage.

Evaluating the activity of AgNPs against adults of *C. maculatus*

The results recorded in Tables 5 and 6 indicate that the using of different AgNP concentrations, which were prepared biologically by both bacterial types, and for several periods, has a high toxicity to the adults of *C. maculatus*. It is noted that, when the insects were treated with *Btt* AgNPs, the highest mortality rate was 58.8% at 3000 ppm, while the lowest mortality rate was 37.5% at 1000 ppm after 72 h, in comparison to the control which was recorded at 20.00%. Regarding the treatments of P.f. AgNPs, where the highest mortality rate was 50.0% with a concentration of 3000 ppm, the lowest mortality was also 50.0% with 1000 ppm. It has been shown to increase mortality by increasing time and concentration. Statistical analysis showed significant differences between the mortality rate when it occurred by *Btt* AgNPs or that which occurred by P.f AgNPs with a preference for *Btt* AgNPs. The % mortality rate increased by concentration with a preference for 3000 ppm concentration. The mortality rate increased over time, both factors gave a significant difference. According to the statistical analysis, no effects have been shown of studied factors on the adult mortality rates.

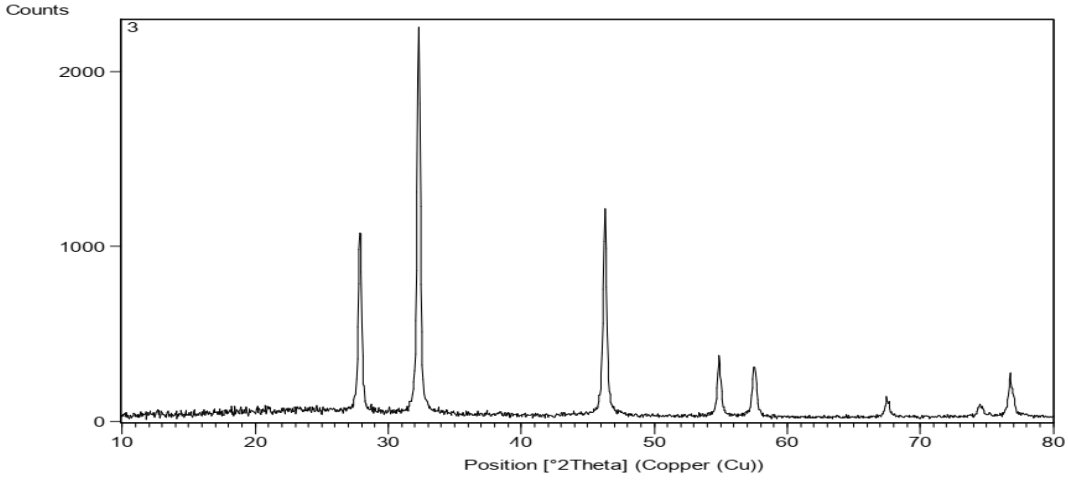

Figure 9. X-ray diffraction of the prepared silver nanoparticles by *Bacillus thuringiensis* subsp. *tenebrionis.*

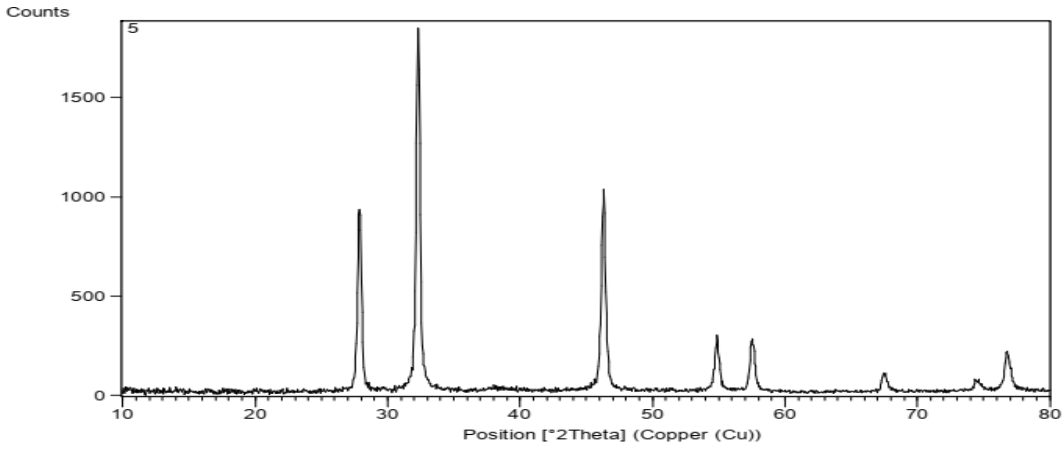

Figure 10. X-ray diffraction of the prepared silver nanoparticles by *Pseudomonas fluorescens.*

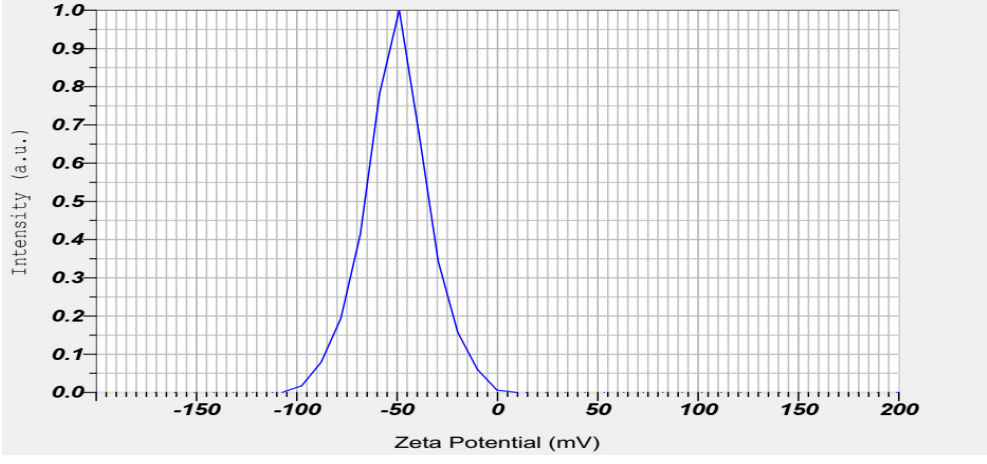

Figure 11. Zeta potential of prepared silver nanoparticles by *Bacillus thuringiensis* subsp. *tenebrionis.*

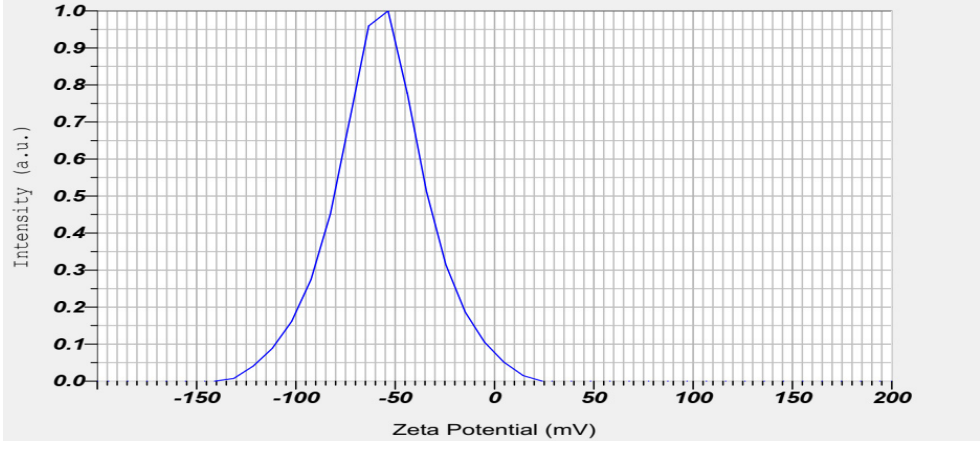

Figure 12. Zeta potential of prepared silver nanoparticles by *Pseudomonas fluorescens***.**

Table 5. Percentage of unhatched eggs of adult southern cowpea beetle *C. maculatus* when treated with different concentrations of silver nanoparticles prepared by *B. thurengenesis* subsp. *tenebrionis* and *P. fluorescens*

Type of SNPS (S)	% Unhitching Eggs				Mean
	Concentration (C) (ppm)				
	1000	2000	3000	Control	
P.f-SNPS	7.7	42.3	53.8	13.3	29.3
Btt-SNPS	11.5	30.8	59.6	13.3	28.8
Mean	9.6	36.5	56.7	13.3	
LSD(P=0.05)	**9.45**				**6.68**
LSD (P=0.05) S×C	**13.37**				

Table 6. Mortality rate for adults of the southern cowpea beetle *Calsobruchus maculatus* at treatment with different concentrations of silver nanoparticles prepared by bacteria *Pseudomonas fluorescens* and *Bacillus thuringiensis* subsp. *tenebrionis*

Type of SNPS (S)	Concentration (C) (ppm)	% Mortality				Mean
		Time (T)				
		24 hrs.	48 hrs.	72 hrs.	96 hrs.	
Btt-SNPS	1000	10.0	16.7	26.7	37.5	26.7
	2000	13.3	30.0	53.3	58.0	
	3000	13.3	40.0	50.0	58.8	
	Control	0.0	0.0	0.0	20.0	
P.f-SNPS	1000	0.0	6.7	14.8	29.2	19.6
	2000	10.0	10.0	44.4	50.0	
	3000	10.0	10.0	44.4	50.0	
	Control	0.0	0.0	10.0	20.0	
Mean (T)		6.7	14.6	30.5	40.9	
LSD (P=0.05)	**6.74**					**4.76**
Mean (C)		1000	2000	3000	Control	
		17.7	33.7	35.0	6.2	
LSD (P=0.05)	**6.74**					
LSD (P=0.05) S×C×T	**19.06**					

DISCUSSION

In a previous study by Backia and Fazila (2014), the highest absorbance of the AgNPs was registered at about 360 nm, this was due to the great ability of reducing agents to accelerate. When Infrared radiation is directed against a compound, each molecule within this compound will absorb energy and become excited, this excitation causes structural changes like folding, twisting, or stretching, the change differs according to the molecule's bonds, so there is a specific absorption for each molecule and this feature is used for diagnosis (Al-Saadi, 2023) the reduction process. We noticed that the particle diameters were larger than their crystal sizes. This is very logical and corresponds to the fact that the diameter must be greater or equal to the crystal size because the crystal size is a part of the total size. The size of the NPs plays a role in their quality and efficiency because the smaller the particle size, the more effective the surface area, and the higher the number of free electrons and lower the bounded electrons, thus the reaction speed increases and its effectiveness exceeds that of their ordinary particles. The stability of nanoparticles depends on many factors, including the concentration of silver nitrate and the concentration of reducing agents, in addition to various conditions such as temperature, pH, reaction time, storage conditions, and exposure to oxidizing agents. It should be noted that when zeta potential is greater than -30 millivolts, this indicates high stability; in contrast, if zeta potential is less than -30, it indicates low stability and a tendency to form clusters, as well as a low nano property potential (Al-Saadi, 2021).

It is believed that AgNPs can penetrate the eggs and kill the embryos, or they may surround the eggs and block gas exchange (Benelli, 2018). The effect of silver nanoparticles has been confirmed in a previous study by Mohamed and Aswad (2019), and the hatching percentage decreased by 49% at 1000 ppm in comparison to the control which was 86.9%. Other studies also supported the possibility of using nanomaterials as insecticides, in combating *C. maculatus* and their eggs (Rouhani *et al*., 2013). It is believed that the effectiveness of AgNPs comes from their ability to detect different body barriers of the insect and bind to some vital molecules, AgNPs can affect the activity of various enzymes, either by binding to the substrate hindering the attachment of enzyme particles or by binding to the enzyme itself and disrupting its work, as well as NPs may cause damage to the plasmic membrane and defect its efficiency (Mao *et al*., 2018). In a similar previous study, the effect of silver nanoparticles prepared by *Btt* and P.f. on cellulase enzymes of ground insects was demonstrated (Kamil *et al*., 2022). The biologically prepared silver nanoparticles showed effectiveness against *C. maculatus* adults with a mortality rate of 71.66% at 2000 ppm (Rouhani *et al.*, 2013) and the lethal concentration LC_{50} was 2.06 g/kg cowpea. The effectiveness of silver nanoparticles in inducing mortality in insect pests is believed to be a result of the particles' ability to penetrate various barriers in the insect's body, reaching the target site and interacting with vital molecules such as enzymes. This interaction affects the efficiency of different enzymes in the insect's body by either binding with the active site and preventing the enzyme from binding to its substrate, or by inhibiting the enzyme's activity through particle-enzyme interactions, as well as causing various effects on the insect's plasmic membrane and affecting its efficiency (Mao *et al.*, 2018). A similar study observed the impact of silver nanoparticles prepared by *Btt* and Ps bacteria on cellulase enzymes in termites (Kamel *et al.*, 2022). The results of the current study align with those of Annon and Jafar (2020), which found that biologically prepared silver nanoparticles were effective in affecting the common bean weevil, causing a mortality rate of 71.66% at a concentration of 2000. Furthermore, Rouhani *et al.* (2013) indicated that the lethal concentration LC_{50} of silver nanoparticles used against the common bean weevil was 2.06 g/kg of beans.

CONCLUSION

The current study revealed the efficiency of biological control by silver nanoparticle produced using bacterial extracts of *Bacillus thuringiensis* subsp. *tenebrionis* and *Pseudomonas fluorescens* which was a safe and environmental friendly method. The prepared NPs characterized by a distinctive property, showed a high efficiency in reducing hatched eggs and killing *C. maculatus* adults. So the experiment of preparing AgNPs from bacterial extracts is a safe and future-promising method for insect control.

ACKNOWLEDGEMENTS

The work has been undertaken as part of the master's degree research programme and demand-driven project at the Department of Biology, Education College, Al-Iraqia University, Iraq and the Ministry of Science and Technology, Integrated Pest Control Center, Iraq. The first author is extremely thankful for providing scientific and laboratory facilities for conducting the work.

REFERENCES

Abbott, W. S. 1925. A method of computing the effectiveness of an insecticide. *J Econ Entom*, **1**(18): 265-267. https://doi.org/10.1093/jee/18.2.265a

Al-Saadi, A. K. 2021. Diagnosis and Characterization of Nanomaterial's. Prince's house.

Al-Saadi, A. K. 2023. Basics of nanomaterials. Dar Al-Yamama.

Al-Saeedi, H. M. L. 2019. Ecology, biology, and evaluation of some pest management methods of longhorn date palm stem borer, Jebusaea hammerschmidtii (Coleoptera: Cerambycidae). Ph.D. Dissertation, University of Baghdad, Iraq.

Annon, M. R., and Jafar, F. S. 2020. The effectiveness of silver and silica nanoparticles on productivity and adult emergence of *T. castaneum* and *C. maculatus*. *J Phys Conf Ser*, **1664**: Article 012110. https://doi.org/10.1088/1742-6596/1664/1/012110

Arora, S., and Srivastava, C. 2020. Locational dynamics of concentration and efficacy of phosphine against pulse beetle *Callosobruchus maculatus* (Fab). *Crop Prote*, **14**: Article 105475. https://doi.org/10.1016/j.cropro.2020.105475

Benelli, G. 2018. Mode of action of nanoparticles against insects. *Environ Sci Pollut Res*, **25**(1): 1-13. https://doi.org/10.1007/s11356-018-1850-4 PMid:29611126

Dakhil, A. S. 2017. Biosynthesis of silver nanoparticle (AgNPs) using lactobacillus and their effects on oxidative stress biomarkers in rats. *J King Saud Univ Sci*, **29**: 462-467. https://doi.org/10.1016/j.jksus.2017.05.013

Kalpna, H. Y. A., and Kumar, R. 2022 .Management of stored grain pest with special reference to *Callosobruchus maculatus*, a major pest of cowpea: A review. *Heliyon*, **8**(1): Article e08703. https://doi.

org/10.1016/j.heliyon.2021.e08703 PMid:35036600 PMCid:PMC8749198

Khan, M., Shaik, M. R., Adil, S. F., Khan, S. T., Al-Warthan, A. A., Siddiqui, M. R. H., Tahir, M. N., Tremel, W., and Siddiqui, R. H. 2018. Plant extracts as green reductants for the synthesis of silver nanoparticles: Lessons from chemical synthesis. *Dalton Trans*, **47**: 11988-12010. https://doi.org/10.1039/C8DT01152D PMid:29971317

Majhi, P. K., and Mogali, S. C. 2020. Characterization and selection of bruchid (*Callosobruchus maculatus* (F.)) tolerant greengram (*Vigna radiata* (L.) Wilczek) genotypes. *Indian J Agric Res*, **54**(6): 679-688.

Malaikozhundan B, and Vinodhini J. 2018. Biological control of the pulse beetle, *Callosobruchus maculatus* in stored grains using the entomopathogenic bacteria, *Bacillus thuringiensis*. *Microb Pathog*, **114**: 139-146. https://doi.org/10.1016/j.micpath.2017.11.046 PMid:29191706

Mao, B. H., Chen, Z. Y., Wang, Y-J., and Yan, S. J. 2018. Silver nanoparticles have lethal and sublethal adverse effects on development and longevity by inducing ROS-mediated stress responses. *Sci Rep*, **8**: Article 2445. https://doi.org/10.1038/s41598-018-20728-z PMid:29402973 PMCid:PMC5799281

Neto E. P. de S., Andrade, A. B. A. de A., Costa, E. M., Maracajia, P. B., Santos, A. B., Santos, J. L. G., and Pimenta, T. A. 2019. Effect of neem powder (*Azadirachta indica A. Juss*) on the control of cowpea weevils (*Callosobruchus maculatus* (F.) (Coleoptera: Bruchidae)] in cowpea beans. *J Exp Agric Int,* **30**(2): 1-7. https://doi.org/10.9734/JEAI/2019/46051

Pisa, L., Goulson, D., Yang, E. C., Gibbons, D., Sánchez-Bayo, F., Mitchell, E., Bonmatin J.-M. 2021. An update of the Worldwide Integrated Assessment (WIA) on systemic insecticides. Part 2: Impacts on organisms and ecosystems. *Environ Sci Pollut Res*, **28**: 11749-11797. https://doi.org/10.1007/s11356-017-0341-3 PMid:29124633 PMCid:PMC7921077

Rouhani, M., Samih, M., and Kalantari, S. 2013. Insecticidal effect of silica and silver nanoparticles on the cowpea seed beetle, *Callosobruchus maculatus* F. (Col.: Bruchidae). *J Entomol Res*, **4**(4): 297-305.

Sharma, S., and Uttam, K. 2017. Rapid analyses of stress of copper oxide nanoparticles on wheat plants at an early stage by laser induced fluorescence and attenuated total reflectance Fourier transform infrared spectroscopy. *Vib Spectrosc*, **92**: 135-150. https://doi.org/10.1016/j.vibspec.2017.06.004

Syed, B., Prasad, M. N. N., Dhananjaya B. L., Kumar, K. M., Yallappa, S., and Satish, S. 2016. Endosymbiont synthesis of silver nanoparticles by pseudomonas fluorescens CA 417 and their bactericidal activity. *Enzyme Microb Technol*, **95**: 128-136. https://doi.org/10.1016/j.enzmictec.2016.10.004 PMid:27866607

Thuy, N. T. T., Huy, L. H., Vy, T. T., Tam, N. T. T., Thanh, B. T. L., and Lan, N. T. M. 2021. Green synthesis of silver nanoparticles using *Plectranthus amboinicus* leaf extract for preparation of CMC/PVA nanocomposite film. *J Renew Mater*, **9**(8): 1393-1411. https://doi.org/10.32604/jrm.2021.015772